Supporting Information

Insight into understanding magnetic transition quite sensitive to nonmagnetic impurity in a one-dimensional S = ½ regular linear chain system

Dong-Sheng Shao,[a] Wan-Wan Yao,[a] Jin Zhang,[a] Yin Qian,*[a] Xiao-Ming Ren*[a,b,c]

[a] State Key Laboratory of Materials-Oriented Chemical Engineering and College of Chemistry and Molecular Engineering, Nanjing Tech University, Nanjing 211816, P. R. China

[b] College of Materials Science and Engineering, Nanjing Tech University, Nanjing 211816, P. R. China

[c] State Key Laboratory of Coordination Chemistry, Nanjing University 210023, P. R. China

Tel: 86-25-58139476

E-mail: yinqian@njtech.edu.cn (YQ); xmren@njtech.edu.cn (XMR)

Contents

Figure S6. EPR experimental and simulation spectra of $[CN\text{-}BzPy]_2[Cu(mnt)_2]$ and $[CN\text{-}BzPy][Cu_xNi_{1-x}(mnt)_2]$ (x = 0.23, 0.34, 0.47 and 1) solid solutions at ambient temperature.

Figure S7: Experimental and fitted χ_m–T plots of $[CN\text{-}BzPy][Cu_xNi_{1-x}(mnt)_2]$ (x = 0.005, 0.01, 0.03, 0.07, 0.12, 0.23, 0.34 and 0.47).

References

Experimental section

Reagents and materials

$CuCl_2 \cdot 2H_2O$, $NiCl_2 \cdot 6H_2O$, iodine and other chemicals used in this work were purchased from commercial sources. Na_2mnt (mnt^{2-} = maleonitriledithiolate), 1-(4'-cyanobenzyl)pyridinium chloride ([CN-BzPy]Cl) and [CN-BzPy][Ni(mnt)$_2$] were prepared following the reported procedures in the literature.[1]

Synthesis of [CN-BzPy][Cu(mnt)$_2$]

[CN-BzPy][Cu(mnt)$_2$] was prepared by a similar process for preparation of [CN-BzPy][Ni(mnt)$_2$], only instead of $NiCl_2 \cdot 6H_2O$ by $CuCl_2 \cdot 2H_2O$. In a 250 mL conical flask, $CuCl_2 \cdot 2H_2O$ (0.17 g, 1 mmol) and Na_2mnt (0.37 g, 2 mmol) were mixed in 15 mL of methanol with stirring for 2 h at ambient temperature, and then filtered. The filtrate was added to a methanol solution (10 mL) containing [CN-BzPy]Cl (0.46 g, 2 mmol) drop by drop, and red microcrystals form immediately. This mixture was further stirred for 2h, and filtered by suction. The microcrystals were washed by 15 mL methanol three times (5 mL per time), and dried in air to obtain [CN-BzPy]$_2$[Cu(mnt)$_2$]. Yield: ca. 75% (calculation based on the reactant $CuCl_2 \cdot 2H_2O$). Elemental Microanalysis calculated for $C_{21}H_{11}CuN_6S_4$ (%): C, 46.78; H, 2.06; N, 15.59 and found: C, 47.08; H, 2.20; N, 15.64.

The methanol solution (10 mL) containing I_2 (0.153 g, 0.6 mmol) was slowly added into the methanol solution (15 mL) with [CN-BzPy]$_2$[Cu(mnt)$_2$] (0.73 g, 1 mmol), the mixture was stirred for 30 min and then black product was harvest by filtration, washed with methanol (5 mL×3 times), and dried under vacuum at ambient temperature. Yield: ca. 75% (calculation based on the reactant $CuCl_2 \cdot 2H_2O$). Elemental Microanalysis calculated for $C_{21}H_{11}CuN_6S_4$ (%): C, 46.78; H, 2.06; N, 15.58 and found: C, 47.08; H, 2.20; N, 15.64. Characteristic IR spectroscopy bands (KBr pellet, cm^{-1}): 3071(w) is attributed to ν_{C-H} of the phenyl ring; 2215(vs) is assigned to $\nu_{C\equiv N}$ of the mnt^{2-} ligands; 1632(s) is attributed to the $\nu_{C=N}$ of the pyridyl ring and the $\nu_{C=C}$ of the phenyl ring; 1515(s) and 1482 (w) arise from $\nu_{C=C}$ of the mnt^{2-} ligands; 1156 (vs) arise from $\nu_{C-S} + \nu_{C-C}$ and $\nu_{C=C}$ of mnt^{2-} ligands.

Syntheses of [CN-BzPy][$Cu_xNi_{1-x}(mnt)_2$] (x = 0.005–0.47)

The solid solutions, [CN-BzPy][$Cu_xNi_{1-x}(mnt)_2$] (x = 0.005–0.47), were prepared using similar procedure. In general, [CN-BzPy][$Cu(mnt)_2$] and [CN-BzPy][$Ni(mnt)_2$] with a molar ratio of $x/(1–x)$ were mixed and dissolved in acetonitrile to give a solution, which was evaporated at ambient temperature for 3–4 days, yielding the crystals of [CN-BzPy][$Cu_xNi_{1-x}(mnt)_2$] (x = 0.005, 0.01, 0.03, 0.07, 0.12, 0.23, 0.34 and 0.47) with yield of more than 90%. The exact x value in each solid solution was determined by ICP technique, and the composition of each solid solution was also characterized by microanalysis for C, H and N elements.

Chemical and Physical Characterizations

Elemental analyses (C, H and N) were performed with an Elementar Vario EL III analytic instrument. Inductively coupled plasma-mass spectrometry (ICP-MS) analyses were performed by a PHI 5000 VersaProbe icp spectrometer. Fourier transform infrared (FTIR) spectra were recorded at ambient temperature on a Nicolet iS5 spectrometer (as KBr pellets) in the spectral regime of 4000–400 cm^{-1}. Raman spectroscopy was collected in the spectral regime of 23—2500 cm^{-1} equipped with a 785 nm laser source (Thermo Fisher Scientific DXR2). Powder X-Ray diffraction (PXRD) data were collected on a Riga-Ku/max-2550 diffractometer with Cu-Kα radiation source (λ = 1.5418 Å) with a step size of 0.02 ° in 2θ angles at ambient temperature. Thermal gravimetric analyses (TGA) were performed by a DTA-TGA 2960 thermogravimetric analyzer under nitrogen atmosphere with the heating rate of 10 °C/min from room temperature to 600 °C. X-band Electron Paramagnetic Resonance (EPR) spectroscopy were performed on a Bruker EMX spectrometer with near 9.7 GHz at ambient temperature. Magnetic susceptibility data were measured for polycrystalline samples by using a Quantum Design MPMS-5 superconducting quantum interference device (SQUID) magnetometer, with temperature range of 2−300 K. The diamagnetism susceptibility was not been deducted from the collected data.

X-ray single crystallography

Single crystal X-Ray diffraction (SCXRD) data were collected on a Bruker D8 QUEST Apex III CCD area detector diffractometer and using the Graphite monochromated Mo-Kα radiation source (λ = 0.71073 Å). Data reduction and absorption correction were performed with the SAINT[2] and SADABS[3] software packages, respectively. All structures were solved by using the SHELXL-2014 software package.[4] The non-hydrogen atoms were anisotropically refined by the full-matrix least-squares method on F^2. All hydrogen atoms were geometrically fixed and placed in ideal position. The site occupation factor of Cu/Ni in the crystal structure of each solid solution was fixed as the value acquired from ICP measurement. The details about crystallography and structure refinement are listed in Table S1.

Details of overlap integral calculation

The overlap integrals (*S*) of the nearest neighboring dimer was calculated by DFT method using Gaussian09[5] and Multiwfn[6] programs. The non-modelized molecular geometry was directly taken from X-ray single crystal structure analysis and no molecular structure optimization was made in our calculations. The popular hybrid exchange-correlation functional B3LYP, which is composed of the Becke's three-parameter hybrid exchange functional[7] and LYP[8] correlation functional as well as the lanl2dz relativistic effective core potential basis set.[9–12] The SCF convergence criterion is 10^{-8}.

Table S1: Crystallographic data and structure refinement parameters for [CN-BzPy][$Cu_xNi_{1-x}(mnt)_2$] (x = 0, 0.005, 0.01, 0.03, 0.07, 0.12, 0.23, 0.34, 0.47 and 1)

	x = 0	x = 0.005	x = 0.01	x = 0.03
CCDC	186340	2162962	2162963	2008202
Temp. / K	293(2)	293(2)	293(2)	293(2)
Formula	$C_{21}H_{11}N_6NiS_4$	$C_{21}H_{11}Cu_{0.005}N_6Ni_{0.995}S_4$	$C_{21}H_{11}Cu_{0.01}N_6Ni_{0.99}S_4$	$C_{21}H_{11}Cu_{0.03}N_6Ni_{0.97}S_4$
Formula weight	534.31	534.33	534.36	534.45
Crystal system	monoclinic	monoclinic	monoclinic	monoclinic
Wavelength/ Å	0.71073	0.71073	0.71073	0.71073
Space group	$P2_1/c$	$P2_1/c$	$P2_1/c$	$P2_1/c$
a / Å	15.197(3)	15.2185(15)	15.2201(9)	15.218(3)
b / Å	17.796(4)	17.8032(18)	17.8167 (10)	17.811(3)
c / Å	8.6089(17)	8.6200(10)	8.6161(5)	8.6127(14)
α / °	90	90	90	90
β / °	95.15(3)	95.1670(3)	95.1822(19)	95.158(5)
γ / °	90	90	90	90
V(Å^3) / Z	2318.9(8)/4	2326.0(4) /4	2326.9(2) /4	2324.9(7) /4
ρ / g cm^{-3}	1.530	1.526	1.525	1.527
F(000)	1084	1084	1084	1084
θ Ranges (data collection °)	3.48-27.49	2.634-27.528	2.635-27.527	2.688-27.487
Index range	-19 ≤ h ≤ 19, -23 ≤ k ≤ 23, -11 ≤ l ≤ 11	-19 ≤ h ≤ 19, -23≤ k ≤ 19, -11 ≤ l ≤ 11	-19 ≤ h ≤ 19, -23 ≤ k ≤ 19, -11 ≤ l ≤ 11	-19 ≤ h ≤ 19, -23 ≤ k ≤ 22, -11 ≤ l ≤ 10
Goodness-of-fit on F^2	1.024	1.011	1.111	1.057
[a] R_1, [b] wR_2 [I>2σ(I)]	R_1 = 0.0332, wR_2 = 0.0733	R_1 = 0.0447, wR_2 = 0.0878	R_1 = 0.0457, wR_2 = 0.0941	R_1 = 0.0774, wR_2 = 0.1057
R_1, wR_2 [all data]	R_1 = 0.0582, wR_2 =0.0835	R_1 = 0.0747, wR_2 = 0.1048	R_1 = 0.0751, wR_2 = 0.1146	R_1 = 0.1703, wR_2 = 0.1279

[a] $R_1 = \sum||Fo| - |Fc|/\sum|Fo|$; [b] $wR_2 = \{\sum[w(Fo^2 - Fc^2)^2]/\sum[w(Fo^2)^2]\}^{1/2}$

contine to Table S1

	x = 0.07	x = 0.12	x = 0.23	x = 0.34
CCDC	2008204	2008203	2008205	2008206
Temp. / K	293(2)	293(2)	293(2) K	293(2) K
Formula	$C_{21}H_{11}Cu_{0.07}N_6Ni_{0.93}S_4$	$C_{21}H_{11}Cu_{0.12}N_6Ni_{0.88}S_4$	$C_{21}H_{11}Cu_{0.23}N_6Ni_{0.77}S_4$	$C_{21}H_{11}Cu_{0.34}N_6Ni_{0.66}S_4$
Formula weight	534.65	534.89	535.42	535.95
Crystal system	monoclinic	monoclinic	monoclinic	monoclinic
Wavelength/ Å	0.71073	0.71073	0.71073	0.71073
Space group	$P2_1/c$	$P2_1/c$	$P2_1/c$	$P2_1/c$
a / Å	15.2144(11)	15.2192(10)	15.2053(16)	15.2328(6)
b / Å	17.8157(12)	17.8077 (10)	17.803(2)	17.7787(7)
c / Å	8.6191(6)	8.6201(6)	8.6092(10)	8.6132(3)
α / °	90	90	90	90
β / °	95.1690(2)	95.180(2)	95.200(3)	95.3120(10)
γ / °	90	90	90	90
V(Å^3) / Z	2326.8(3) /4	2326.7(3) /4	2321.0(5) /4	2322.60(15)/4
ρ / g cm^{-3}	1.526	1.527	1.532	1.533
F(000)	1084	1084	1085	1085
θ Ranges (data collection °)	2.634-27.495	2.634-27.522	2.861-27.514	2.637-27.526
Index range	-19 ≤ h ≤ 16, -23≤ k ≤ 23, -11 ≤ l ≤ 11	-19 ≤ h ≤ 19, -23 ≤ k ≤ 19, -9 ≤ l ≤ 11	-16 ≤ h ≤ 19, -23 ≤ k ≤ 22, -11 ≤ l ≤ 9	-19 ≤ h ≤ 19, -23 ≤ k ≤ 18, -11 ≤ l ≤ 11
Goodness of fit on F^2	1.178	1.026	1.089	1.008
[a] R_1, [b] wR_2 [I>2σ(I)]	R_1 = 0.0487, wR_2 = 0.1284	R_1 = 0.0421, wR_2 = 0.0770	R_1 = 0.0479, wR_2 = 0.0852	R_1 = 0.0380, wR_2 = 0.0771
R_1, wR_2 [all data]	R_1 = 0.0873, wR_2 = 0.1661	R_1 = 0.0956, wR_2 = 0.0949	R_1 = 0.0957, wR_2 = 0.1025	R_1 = 0.0849, wR_2 = 0.0899

[a] $R_1 = \sum||Fo| - |Fc|/\sum|Fo|$; [b] $wR_2 = \{\sum[w(Fo^2 - Fc^2)^2]/\sum[w(Fo^2)^2]\}^{1/2}$

contine to Table S1

	x = 0.47	x = 1
CCDC	2008200	2008201
Temp. / K	293(2)K	293(2)K
Formula	$C_{21}H_{11}Cu_{0.47}N_6Ni_{0.53}S_4$	$C_{21}H_{11}CuN_6S_4$
Formula weight	536.58	539.14
Crystal system	monoclinic	monoclinic
Wavelength/ Å	0.71073	0.71073
Space group	$P2_1/c$	$P2_1/c$
a / Å	15.2877(9)	15.2254(5)
b / Å	17.7606(10)	17.8123(6)
c / Å	8.6077(5)	8.6152(3)
α / °	90	90
β / °	95.554(2)	95.1890(10)
γ / °	90	90
V(Å^3) / Z	2326.2(2)/4	2326.86(14)/4
ρ / g cm^{-3}	1.532	1.539
F(000)	1086	1088
θ Ranges (data collection °)	2.640-27.505	3.478-27.493
Index range	-19 ≤ h ≤ 19, -23 ≤ k ≤ 19, -11 ≤ l ≤ 8	-18 ≤ h ≤ 19, -23 ≤ k ≤ 23, -11 ≤ l ≤ 11
Goodness-of-fit on F^2	0.942	1.486
[a] R_1, [b] wR_2 [I>2σ(I)]	R_1 = 0.0496, wR_2 = 0.1037	R_1 = 0.0585, wR_2 =0.1882
R_1, wR_2 [all data]	R_1 = 0.1281, wR_2 = 0.1312	R_1 = 0.0901, wR_2 =0.2185

[a] $R_1 = \sum||Fo| - |Fc|/\sum|Fo|$; [b] $wR_2 = \{\sum[w(Fo^2 - Fc^2)^2]/\sum[w(Fo^2)^2]\}^{1/2}$

Table S2: Selected bond parameters for [CN-BzPy][$Cu_xNi_{1-x}(mnt)_2$] (x = 0, 0.005, 0.01, 0.03, 0.07, 0.12, 0.23, 0.34, 0.47 and 1)

	x = 0	x = 0.005	x = 0.01	x = 0.03
		Bond distances		
M…M	4.517	4.544	4.543	4.542
M(1)–S(1)	2.1388(7)	2.1398(9)	2.1407(9)	2.1427(15)
M(1)–S(2)	2.1495(7)	2.1509(9)	2.1521(9)	2.1468(16)
M(1)–S(3)	2.1471(7)	2.1473(9)	2.1490(9)	2.1490(16)
M(1)–S(4)	2.1493(7)	2.1513(9)	2.1514(9)	2.1554(16)
		Bond angles		
S(1)–M(1)–S(2)	92.50(3)	92.42(3)	92.49(3)	92.55(6)
S(1)–M(1)–S(4)	87.10(3)	87.20(3)	87.17(3)	87.09(6)
S(3)–M(1)–S(2)	87.73(3)	87.83(4)	87.74(4)	87.82(6)
S(3)–M(1)–S(4)	92.69(3)	92.57(3)	92.62(4)	92.56(6)

Continue to Table S2

	x = 0.07	x = 0.12	x = 0.23	x = 0.34
		Bond distances		
M…M	4.544	4.545	4.540	4.545
M(1)–S(1)	2.1413(11)	2.1405(8)	2.1390(10)	2.1520(6)
M(1)–S(2)	2.1512(11)	2.1499(9)	2.1477(10)	2.1441(6)
M(1)–S(3)	2.1504(11)	2.1489(8)	2.1470(10)	2.1537(6)
M(1)–S(4)	2.1517(11)	2.1514(8)	2.1511(10)	2.1512(6)
		Bond angles		
S(1)–M(1)–S(2)	92.54(4)	92.45(3)	92.55(4)	92.52(2)
S(1)–M(1)–S(4)	87.11(4)	87.14(3)	87.01(4)	87.71(3)
S(3)–M(1)–S(2)	87.69(4)	87.82(3)	87.76(4)	87.08(2)
S(3)–M(1)–S(4)	92.67(4)	92.61(3)	92.70(4)	92.69(2)

Continue to Table S2

	x = 0.47	x = 1
	Bond distances	
M…M	4.545	4.543
M(1)–S(1)	2.1575(10)	2.1417(10)
M(1)–S(2)	2.1500(9)	2.1526(10)
M(1)–S(3)	2.1610(9)	2.1493(10)
M(1)–S(4)	2.1555(9)	2.1524(10)
	Bond angles	
S(1)–M(1)–S(2)	92.52(4)	92.49(4)
S(1)–M(1)–S(4)	87.70(4)	87.18(4)
S(3)–M(1)–S(2)	86.97(3)	87.72(4)
S(3)–M(1)–S(4)	92.81(4)	92.62(4)

Table S3: EPR simulation data of [CN-BzPy][$Cu_xNi_{1-x}(mnt)_2$] (x = 0.23, 0.34, 0.47 and 1) and [CN-BzPy]$_2$[Cu (mnt)$_2$]

	[CN-BzPy]$_2$ [Cu (mnt)$_2$]	x = 0.23	x = 0.34	x = 0.47	x = 1
g_x	2.0141	1.9855	1.9961	1.9915	1.9672
g_y	2.0192	2.0225	2.0405	2.0295	2.0434
g_z	2.0842	2.1337	2.1450	2.1395	2.0745
$A_{(x, x)}$	0	0	0	0	32
$A_{(y, y)}$	0	11	5.8	12	38
$A_{(z, z)}$	0	0	0	0	70
S_x	4.4	8	9.6	10	8
S_y	2.5	8	9.6	10	7
S_z	10	15	15	15	12

Note: A and S are representative of hyperfine coupling constant and shape parameters.

Table S4: Fit parameters for magnetic susceptibility of [CN-BzPy][$Cu_xNi_{1-x}(mnt)_2$] (x = 0.005, 0.01, 0.03, 0.07, 0.12, 0.23, 0.34, 0.47 and 1)

x	0.005	0.01	0.03	0.07	0.12
C / emu K mol^{-1}	0.0013	0.0011	0.0026	0.0029	0.00473
Magnetic impurity/%*	0.33	0.25	0.56	0.48	0.75
θ/ K	1.29	1.48	-0.60	-0.20	-0.57
χ_0 / emu mol^{-1}	-1.81×10^{-4}	-4.03×10^{-4}	9.56×10^{-8}	-3.50×10^{-5}	5.23×10^{-5}
Temp. range / K	2–15	2–15	2–80	2–105	2–180

Continue to Table S4

x	0.23	0.34	0.47	1
C / emu K mol^{-1}	0.0409	0.0429	0.0378	0.0158
Magnetic impurity/%*	9.93	9.97	8.13	4.21
θ/ K	-0.49	-0.35	1.50	-0.53
χ_0 / emu mol^{-1}	-1.08×10^{-4}	-1.72×10^{-4}	1.07×10^{-4}	-3.56×10^{-4}
Temp. range / K	2–220	2–300	2–300	2–300

*Notes: Magnetic impurity contributed from the uncoupling spins, which is obtained by the value of C/0.375-4.2%x

Table S5: Selected intermolecular distances between two neighboring NiS_4 cores in [CN-BzPy][Ni(mnt)$_2$] and [NO_2-BzPy][Ni(mnt)$_2$]

	Ni…Ni	Ni…S	S…S
[CN-BzPy][Ni(mnt)$_2$]	4.517	3.629	3.804
[NO_2-BzPy][Ni(mnt)$_2$]	3.807	3.599	3.658

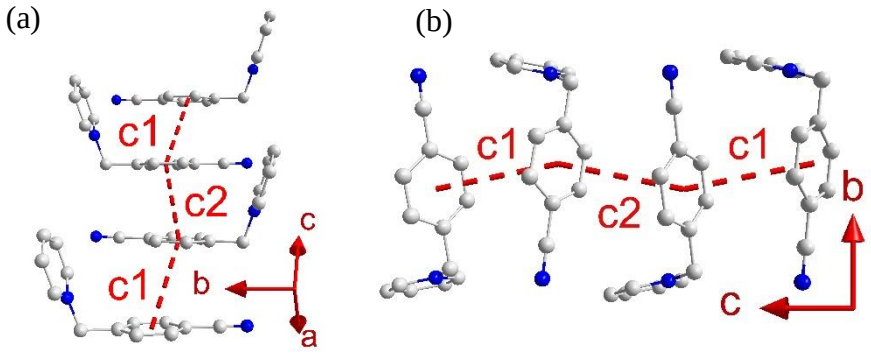

Figure S1: (a) The neighboring cations adopt the boat-type arrangement and (b) the side views of an cation stack along *c* directions in [CN-BzPy][Cu(mnt)$_2$].

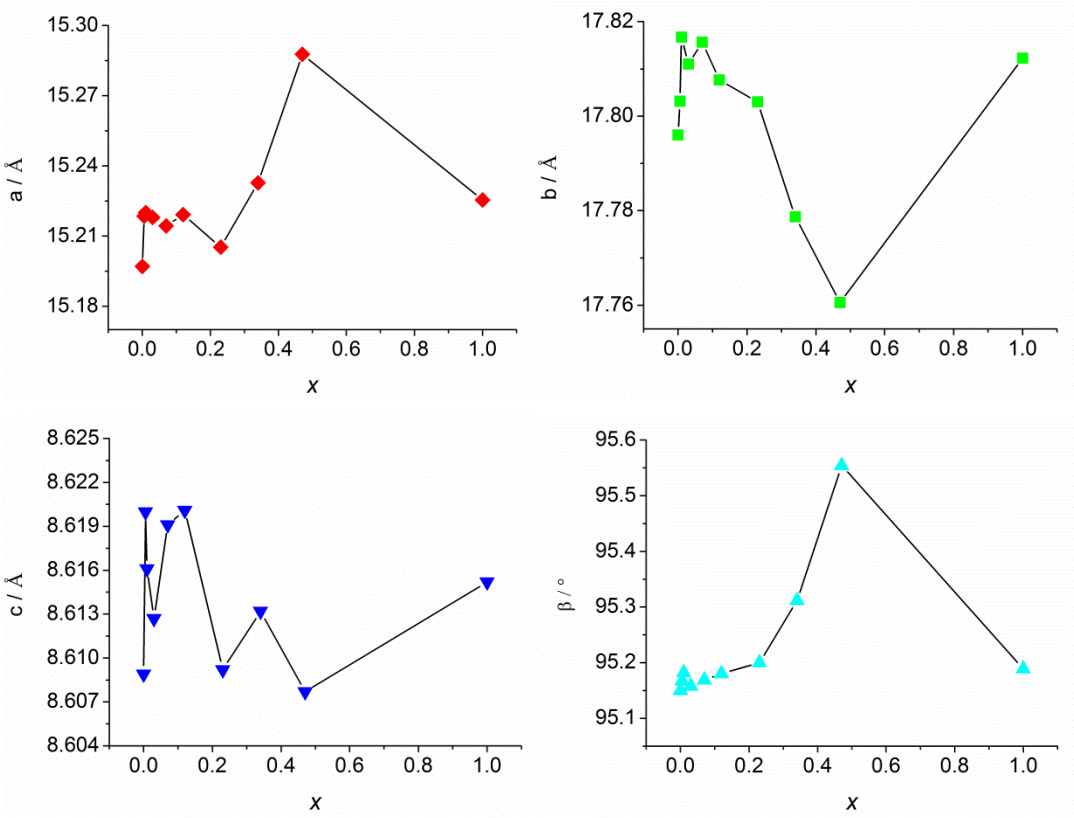

Figure S2: Cell parameters are plotted against *x* of [CN-BzPy][Cu$_x$Ni$_{1-x}$(mnt)$_2$] (*x* = 0–1) at ambient temperature.

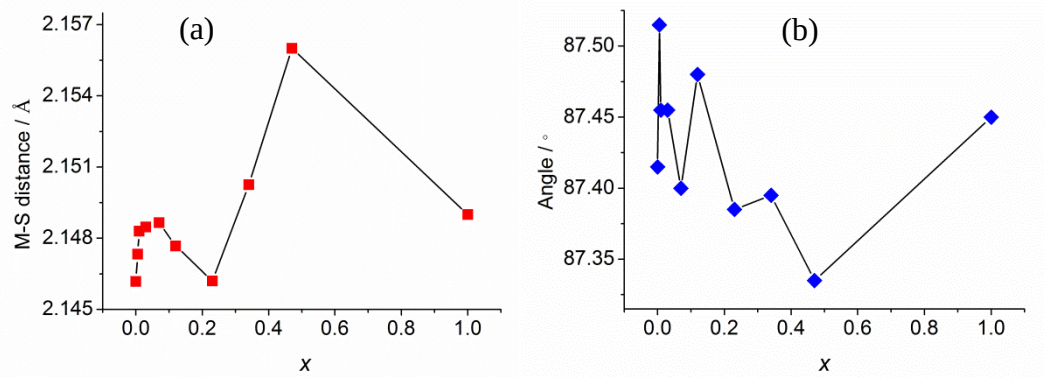

Figure S3: (a) The average bond length of M–S and (b) the average bite angle of ∠S–M–S *versus* the relative content of Cu (*x*) in [CN-BzPy][$Cu_xNi_{1-x}(mnt)_2$] (*x* = 0–1).

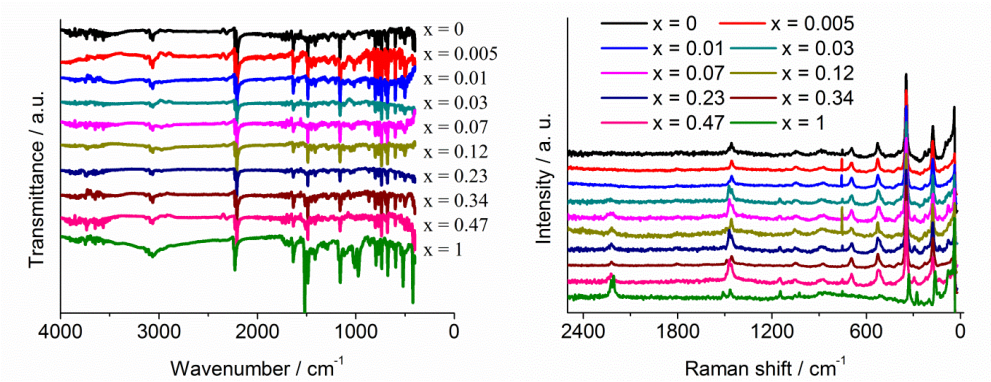

Figure S4: (a) IR spectra (4000–400 cm^{-1}) and (b) Raman spectra (2500–20 cm^{-1}) of [CN-BzPy][$Cu_xNi_{1-x}(mnt)_2$] (*x* = 0–1) at ambient temperature.

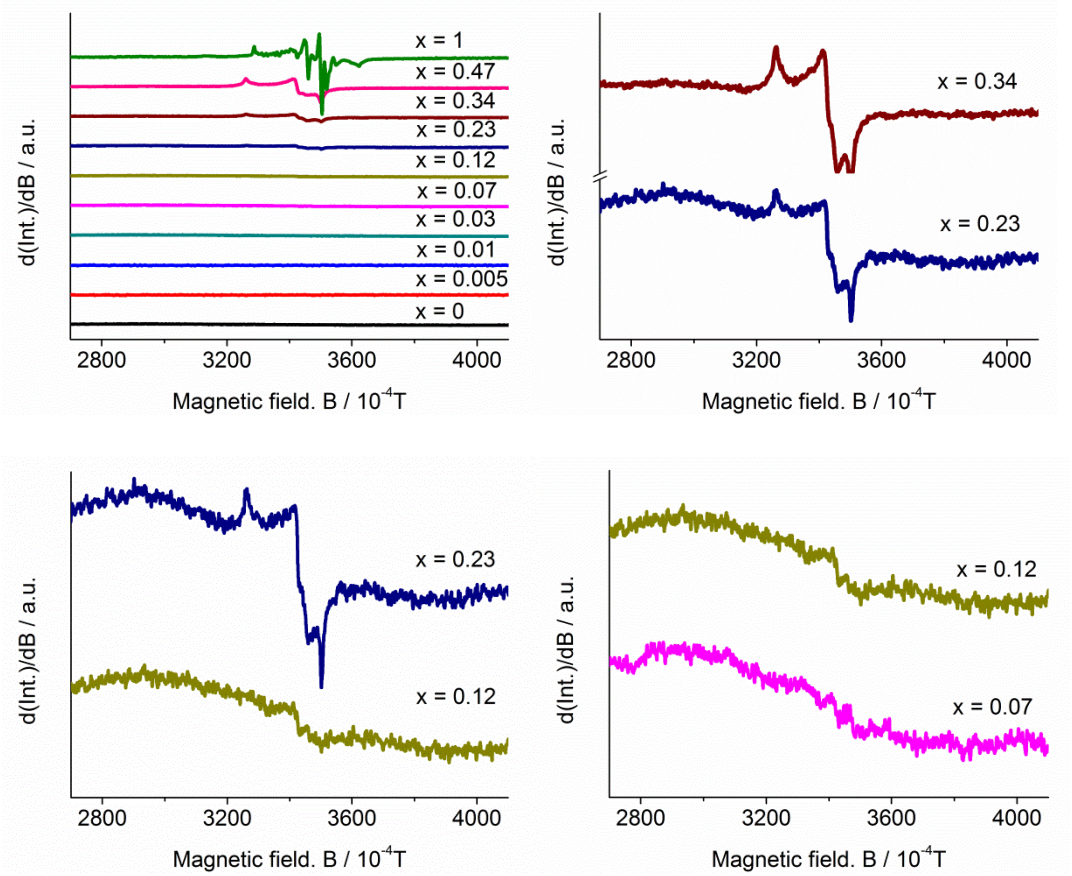

Figure S5: EPR spectra of [CN-BzPy][$Cu_xNi_{1-x}(mnt)_2$] (x = 0, 0.005, 0.01, 0.03, 0.07, 0.12, 0.23, 0.34, 0.47 and 1) at ambient temperature.

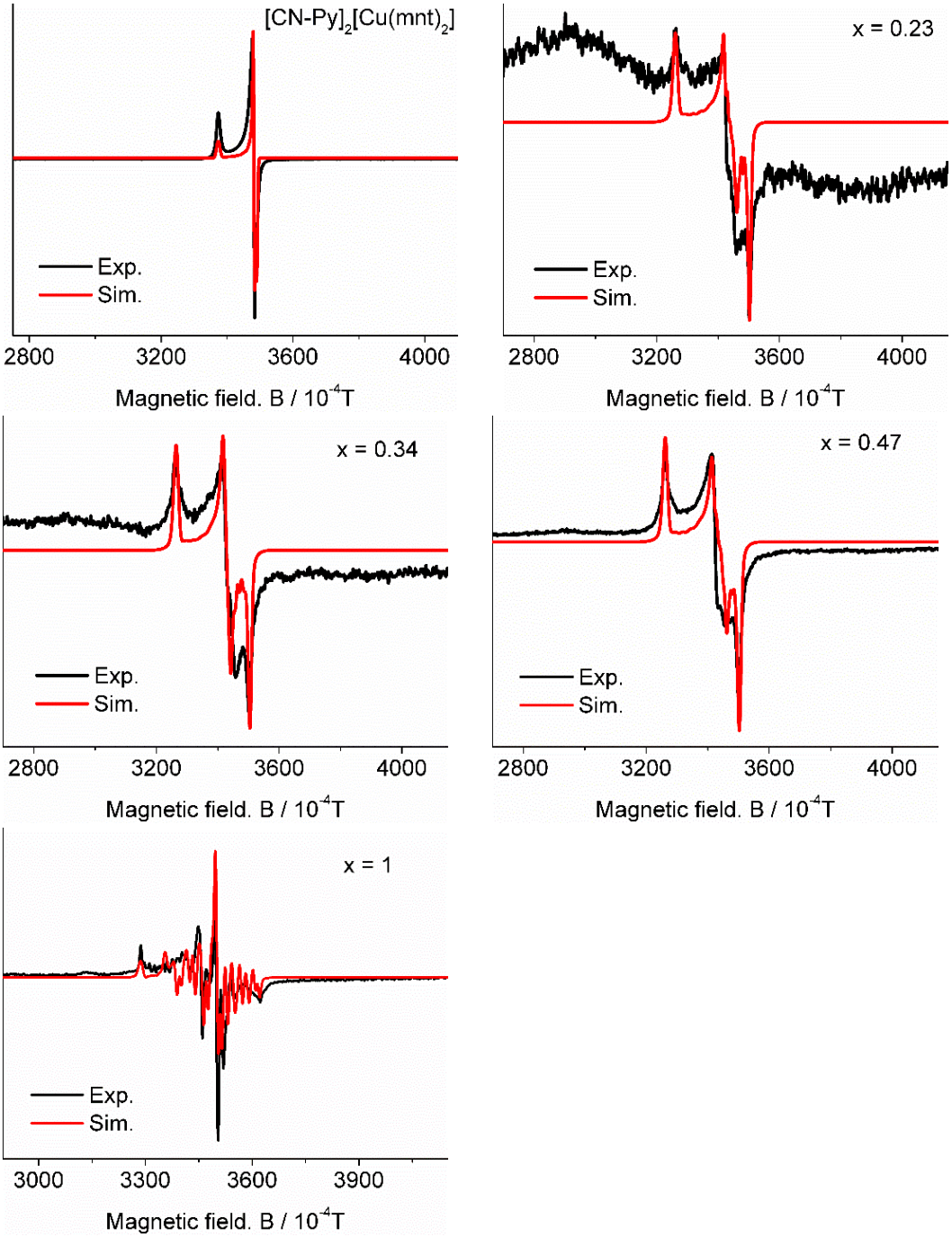

Figure S6. EPR experimental and simulation spectra of $[CN\text{-}BzPy]_2[Cu(mnt)_2]$ and $[CN\text{-}BzPy][Cu_xNi_{1-x}(mnt)_2]$ (x = 0.23, 0.34, 0.47 and 1) solid solutions at ambient temperature.

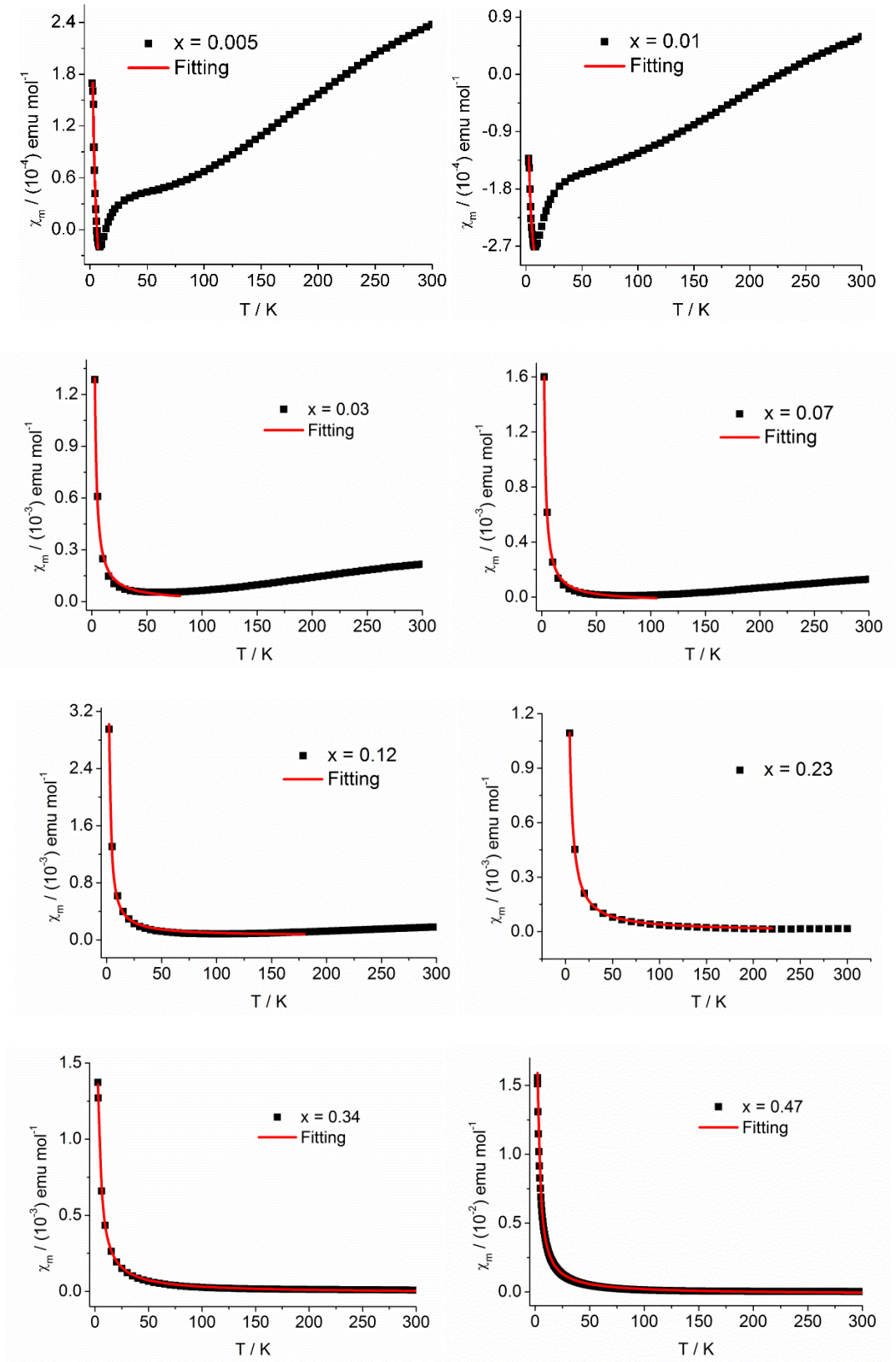

Figure S7: Experimental and fitted χ_m–T plots of [CN-BzPy][$Cu_xNi_{1-x}(mnt)_2$] (x = 0.005, 0.01, 0.03, 0.07, 0.12, 0.23, 0.34 and 0.47).

References

1. J. L. Xie, X. M. Ren, C. He, Y. Song, Q. J. Meng, R. K. Kremer and Y. G. Yao, Complicated magnetic behavior in one-dimensional nickel(III) chain complex [1-(4'-cyanobenzyl)pyridinium][Ni(mnt)$_2$] (mnt^2 = maleonitriledithiolate), *Chem. Phys. Lett.*, 2003, **369**, 41–48.
2. Bruker, *APEX 2*, *SAINT*, *XPREP*, Bruker AXS Inc., Madison, Wisconsin, USA, 2007.
3. Bruker, *SADABS*, Bruker AXS Inc., Madison, Wisconsin, USA, 2001.
4. G. M. Sheldrick, *SHELXS-2014*, Program for the Solution and Refinement of Crystal Structures, University of Göttingen, Göttingen, Germany, 2014.
5. M. J. Frisch, G. W. Trucks, H. B.Schlegel, G. E. Scuseria, M. A. Robb and J. R. Cheeseman, GAUSSIAN 09, Revision A.02, Gaussian Inc, Wallingford, CT, 2009.
6. T. Lu and F. Chen, Multiwfn: A Multifunctional Wavefunction Analyzer, *J. Comput. Chem.*, 2012, **33**, 580−592.
7. A. D. Becke, Density-functional thermochemistry. III. The role of exact exchange, *J. Chem. Phys.*, 1993, **98**, 5648−5652.
8. C. Lee, W. Yang and R. G. Parr, Development of the Colle-Salvetti correlation-energy formula into a functional of the electron density, *Phys. Rev. B*, 1988, **37**, 785–789.
9. T. H. Dunning Jr and P. J. Hay, *Modern Theoretical Chemistry*, Plenum, New York, 1976, 1–28.
10. P. J. Hay and W. R. Wadt, Ab Initio effective core potentials for molecular calculations. Potentials for the transition metal atoms Sc to Hg, *J. Chem. Phys.*, 1985, **82**, 270–283.
11. W. R. Wadt and P. J. Hay, Ab initio effective core potentials for molecular calculations. Potentials for main group elements Na to Bi, *J. Chem. Phys.*, 1985, **82**, 284–298.
12. P. J. Hay and W. R. Wadt, Ab initio effective core potentials for molecular calculations. Potentials for K to Au including the outermost core orbitals, *J. Chem. Phys.*, 1985, **82**, 299–310.